

# Multiplets Matter: The Electronic Structure of Rare-Earth Semiconductors and Semimetals

Leonid V. Pourovskii,<sup>1</sup> Kris T. Delaney,<sup>2</sup> Chris G. Van de Walle,<sup>3</sup> Nicola A. Spaldin,<sup>3</sup> and Antoine Georges<sup>1</sup>

<sup>1</sup>*Centre de Physique Théorique, CNRS, École Polytechnique, 91128 Palaiseau, France*

<sup>2</sup>*Materials Research Laboratory, University of California, Santa Barbara, 93106-5121, USA*

<sup>3</sup>*Materials Department, University of California, Santa Barbara, 93106-5050, USA*

We demonstrate that a theoretical framework fully incorporating intra-atomic correlations and multiplet structure of the localized  $4f$  states is required in order to capture the essential physics of rare-earth semiconductors and semimetals. We focus in particular on the rare-earth semimetal erbium arsenide (ErAs), for which effective one-electron approaches fail to provide a consistent picture of both high and low-energy electronic states. We treat the many-body states of the Er  $4f$  shell within an atomic approximation in the framework of dynamical mean-field theory. Our results for the magnetic-field dependence of the  $4f$  local moment, the influence of multiplets on the photoemission spectrum, and the exchange splitting of the Fermi surface pockets as measured from Shubnikov-de Haas oscillations, are found to be in good agreement with experimental results.

PACS numbers:

The established framework for understanding the electronic structure of many materials is based on independent electrons subject to a self-consistent potential. This description often fails, however, when electronic states associated with localized orbitals are involved. Those states, while being too close in energy to the valence to be considered as ‘core’ states, do keep a strong atomic-like character. For such materials, an entirely different point of view is required, in which intra-atomic correlations and the full multiplet structure are taken into account from the start. Here, we report on a particularly dramatic example: erbium arsenide, a semi-metal involving a partially filled  $4f$  shell. Interest in this compound was initially stimulated by growth, through molecular beam epitaxy, of ErAs onto pseudomorphically compatible III-V semiconductor substrates of zinc-blende structure. The result is a high-quality, epitaxial metallic contact with a continuous anion sublattice through the interface[1]. Other growth modes[1, 2, 3, 4] have been found to yield metallic ErAs nanoparticles epitaxially embedded in the semiconductor matrix, with potential applications including efficient thermoelectrics[5] and solid-state THz emitters[6].

The low-energy electronic states of erbium arsenide (ErAs) consist[1] of a conduction band and a valence band, with predominant Er  $5d$  and As  $4p$  character respectively. The small energy-overlap of these bands is responsible for the semimetallic nature of this material. In contrast, the Er  $4f$  electrons are well localized and form local moments. Treating simultaneously these two kinds of electronic states is a major challenge for conventional electronic structure theories. Indeed, when the  $4f$  states are treated as core electrons, calculations based on the local-density approximation (LDA) do yield a semi-metal, but do not otherwise provide an accurate description of the electronic properties. The volume of the calculated FS pockets is approximately three

times too large, leading to incorrect carrier concentrations and SdH frequencies[7, 8] compared with accurate measurements[9, 10, 11, 12].

Here we show that a proper treatment of the strong correlations and multiplet structure of the  $4f$  shell provides a solution to these difficulties. Our finding is general and has fundamental consequences for the understanding of the electronic structure of a large class of rare-earth compounds. ErAs is a particularly remarkable example, however, in which the electronic states *near the Fermi level* act as a sensitive probe of the atomic physics associated with more strongly bound localized states.

Our approach is based on the dynamical mean-field theory[13] (DMFT), combined[14, 15] with LDA. The  $4f$  shell is treated as that of an effective atom self-consistently coupled to an environment describing the rest of the solid. From the hamiltonian of this effective atom (which takes into account crystal-field effects, intra-atomic Coulomb interactions and the spin-orbit coupling), a many-body self-energy is computed within the Hubbard-I approximation [16] and inserted into the Green’s function of the full solid. Self-consistency over the total charge density and the effective atom parameters is implemented. The full description of our approach can be found in Ref. [17]. In the present work it was generalized to include the spin-orbit interaction as well as the full 4-index local Coulomb interaction matrix. The parameter  $U = 7.94$  eV of the local Coulomb interaction on the Er  $4f$  shell has been determined by constrained LDA calculations, while the Slater integrals  $F^2 = 12.1$  eV,  $F^4 = 8.4$  eV, and  $F^6 = 6.7$  eV, which are known to be weakly dependent on the crystalline environment, have been taken from the optical measurements on Er ions embedded in a  $\text{LaF}_3$  host [18]. To perform LDA+U calculations we have used the same framework, including the spin-orbit interaction, with the Hubbard-I self-energy being substituted by a local self-energy computed within

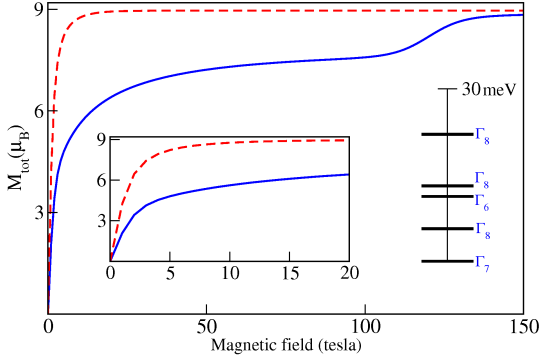


FIG. 1: (Color online) Calculated DMFT total magnetic moment on Er 4f shell vs. applied magnetic field at  $T = 4.2$  K with (solid blue curve) and without (red dashed curve) crystal field effects taken into account. The left inset shows the zoom in the field's range up to 20 T. The crystal field splitting of the  $^4I_{15/2}$  multiplet obtained by LDA+DMFT in paramagnetic ErAs is shown in the right inset.

the rotationally-invariant Hartree-Fock expression. All our calculations have been carried out in the rock-salt structure at the ErAs experimental lattice parameter of 5.74 Å.

The ground-state of an isolated  $\text{Er}^{3+}$  ion ( $4f^{11}5d^0$ ) is a 16-fold degenerate multiplet  $^4I_{15/2}$  ( $S = \frac{3}{2}, L = 6, J = \frac{15}{2}$ ). In a cubic crystal-field and at zero magnetic field, this multiplet is expected to split into twofold degenerate  $\Gamma_6$  and  $\Gamma_7$  multiplets, as well as three 4-fold degenerate  $\Gamma_8$  multiplets [19]. At self-consistency, the zero-field eigenstates of our effective atom hamiltonian (inset of Fig. 1) follow this expectation, the obtained ground-state being the  $\Gamma_7$  multiplet. As a magnetic field  $H$  is turned on, the ground-state remains approximately  $\Gamma_7$  for a wide range of field, and can be decomposed on eigenstates of  $J_z$  according to:  $a_{13/2}^{(H)}|J_z = \frac{13}{2}\rangle + a_{5/2}^{(H)}|J_z = \frac{5}{2}\rangle + a_{-3/2}^{(H)}|J_z = -\frac{3}{2}\rangle + a_{-11/2}^{(H)}|J_z = -\frac{11}{2}\rangle$ , where the coefficients  $a_{J_z}$  depend on magnetic field. The magnetic moment *vs.* field curve (Fig. 1) displays an initial sharp rise due to the Zeeman splitting of the  $\Gamma_7$  state, followed by a rather slow increase in the range from 5 to 120 T due to the progressive polarization of the  $\Gamma_7$  state. From magnetoresistance experiments[12], it was proposed that the magnetic moment is saturated at a value[20]  $\sim 5.3\mu_B$  in fields above 10 T. Indeed, we find values ranging from  $4.8\mu_B$  at  $H = 5$  T to  $5.6\mu_B$  at  $H = 10$  T, in good agreement with the experimental estimate[20]. However, our analysis shows that this is rather a quasi-saturation, with the moment being “frozen” by the crystal field. Eventually, at a very high field  $H \simeq 120$  T we predict a sharp increase of the moment to  $8.9\mu_B$ , corresponding to a symmetry-changing transition of the ground-state from  $\Gamma_7$  to  $\Gamma_8$ .

It is interesting to contrast these findings to those of

LDA+U calculations. We performed these for ferromagnetic ordering since, for fields above  $\sim 1$  T relevant to SdH experiments, this is the observed configuration[20]. In the LDA+U approach [21], Coulomb interaction effects within the 4f-shell are described by a self-consistent, orbital- and spin- dependent, *one-electron potential*. As a result, the LDA+U solution of lowest energy is found to correspond to the filling of independent electron levels according to Hund's rules[22], leading to the highest possible spin and orbital moments consistent with a  $4f^{11}$  shell. Indeed, our LDA+U results yield a spin, orbital and total moment of  $2.9\mu_B$ ,  $6.0\mu_B$ , and  $8.9\mu_B$  respectively, in contradiction with the observed experimental value quoted above. Furthermore, as pointed out by Larson *et al.* for nitrides [22], the LDA+U solution breaks the cubic symmetry of the lattice, because it is constructed by occupying one-electron eigenstates of the angular momentum operator  $\hat{L}_z$ . LDA+U solutions preserving cubic symmetry are obtained by occupying symmetry-adapted one-electron states (which are *not* eigenstates of  $\hat{L}_z$ ), but they have higher energy. Hence, in a one-electron effective description, the system has to choose between minimizing the intra-atomic Coulomb interaction energy and preserving the lattice symmetry. In reality however, this dilemma does not apply since atomic multiplets satisfy both requirements. A proper many-body treatment of atomic correlations avoids this conundrum, as demonstrated above. We now describe the electronic structure of ErAs, obtained with LDA+U and LDA+DMFT (Fig. 2). Distinctive features corresponding to the 4f states are observed at high energy, corresponding to the upper- and lower- Hubbard bands (UHB/LHB). In LDA+DMFT, those “bands” truly are many-body atomic-like excitations associated with the removal (LHB) or addition (UHB) of an electron in the 4f shell. The LHB spans an energy range from  $\sim -11$  eV to  $-5.5$  eV, in agreement with photoemission experiments[23, 24]. Within LDA+DMFT the UHB consists not only of the main peak at 2–3 eV above the Fermi energy, but also of additional multiplet peaks at  $\sim 3–4$  eV. As also discussed for  $\delta$ -Pu[25], this multiplet structure is responsible for the apparent width of the UHB, which we find to be  $\sim 1.5$  eV, in agreement with inverse photoemission measurements [23, 24].

In contrast, the UHB found with LDA+U spans an energy range of only  $\sim 0.75$  eV, because the additional multiplet peaks are missed in this approach. Furthermore, a distinctive feature found within LDA+U is that the UHB is almost fully (minority) spin-polarized. This is clearly due to the maximal (Hund's rule) spin moment, corresponding to the complete filling of the 4f majority-spin states so that no electron addition is possible in the majority channel. In contrast, the UHB found within LDA+DMFT is found to have only partial spin polarization. Hence UHB transitions are possible in both spin channels, a distinctive prediction for possible spin-

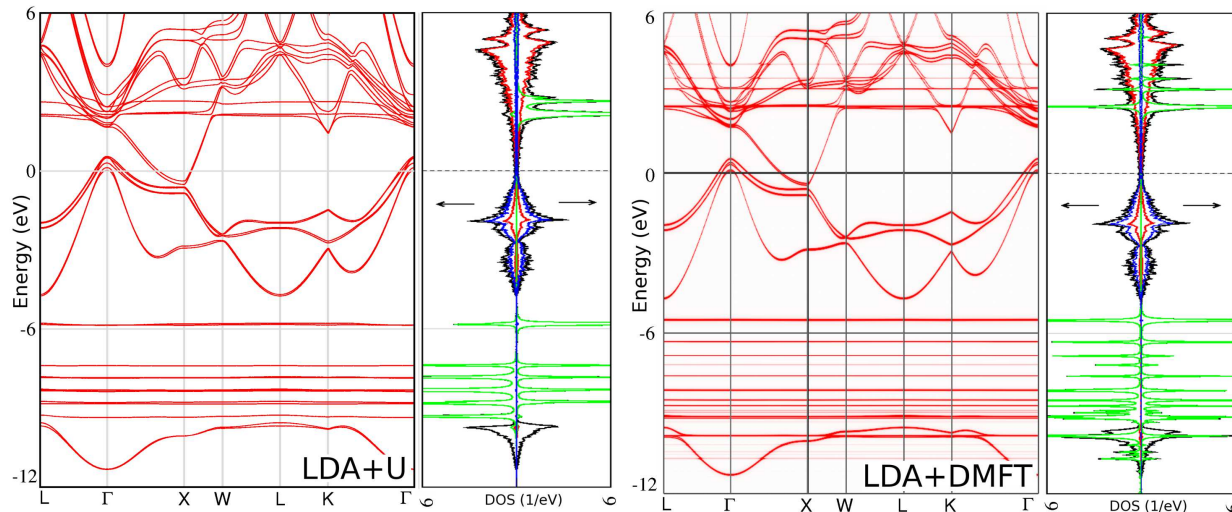


FIG. 2: Band structure and density of states (DOS) of ErAs: from LDA+U (left), and LDA+DMFT at an applied field of 5 T (right). In the corresponding DOS plots the total, Er 5d, Er 4f and As 4p states are displayed by the black, red, green, and blue curves respectively.

TABLE I: Shubnikov-de Haas (SdH) frequencies (in tesla) and carrier concentrations of electrons/holes  $n$  (in  $10^{20}\text{cm}^{-3}$ ). The frequencies  $f_{sh}$ ,  $f_{lh}$ , and  $f_{hh}$  correspond to cross sections of the small, light, and heavy hole pockets near the  $\Gamma$  high-symmetry point, respectively. The frequencies  $e \perp$  and  $e \parallel$  are due to the transverse and longitudinal cross sections of the ellipsoidal electronic pocket. The experimental carrier concentrations and SdH frequencies are for an  $\text{Er}_{0.57}\text{Sc}_{0.43}\text{As}$  alloy [12].

Orbits	Exp.		LDA	LSDA+U		LDA+DMFT	
	$\uparrow$	$\downarrow$	$\uparrow/\downarrow$	$\uparrow$	$\downarrow$	$\uparrow$	$\downarrow$
$f_{sh}$	150	150	511	163	40	140	72
$f_{lh}$	612	589	1590	907	597	619	574
$f_{hh}$	1273	1222	2479	1592	1907	1637	1466
$f_{e\perp}$	386	328	479	333	243	362	306
$f_{e\parallel}$	1111	941	1848	1205	850	1270	1113
$n$	3.3		7.6	4.1		3.9	

polarized photoemission experiments.

We now show that these differences in the description of the high-energy 4f states have key consequences for the electronic properties of states near the Fermi level. Near the  $\Gamma$  high-symmetry point, the As 4p bands form “heavy-” ( $hh$ ) and “light-” ( $lh$ ) hole pockets, as well as a small hole pocket ( $sh$ ) due to the spin-orbit splitting of the 4p states, while the ellipsoidal electronic pocket at the X-point is associated with the Er 5d- states (Fig. 3). As mentioned above, a conventional LDA approach treating the 4f shell as core states severely overestimates the  $p$ - $d$  overlap, and hence the carrier concentration and the size of the FS pockets. Both the LDA+DMFT and LDA+U

TABLE II: Exchange splittings of Shubnikov-de Haas frequencies  $\Delta = f^{\uparrow} - f^{\downarrow}$  (in tesla)

Orbits	Experiment <sup>a</sup>	LSDA+U	GW <sup>b</sup>	LDA+DMFT
$\Delta_{lh}$	23	310	136	45
$\Delta_{hh}$	51	315	274	171
$\Delta_{e\perp}$	58	90	151	56
$\Delta_{e\parallel}$	170	355	430	157

<sup>a</sup>Experimental data for an  $\text{Er}_{0.57}\text{Sc}_{0.43}\text{As}$  alloy [12].

<sup>b</sup>Chantis *et al.* [27]

treatment of the 4f states lead to a drastic reduction in the magnitude of the carrier density and SdH frequencies (Table I), and hence to a much better agreement with experiments. These results demonstrate that taking into account interaction effects in the 4f shell is key to a proper description of the *valence* band structure of ErAs. Previous works employed an empirical shift of the 5d band in order to correct for the inadequacies of LDA [8, 26]. Despite the overall reduction in the FS pocket volume, the LDA+U (self-consistent one-electron potential) and LDA+DMFT (self-consistently embedded atom) results differ significantly when it comes to the exchange splitting of these pockets. In Table II, we display the measured splittings [9, 11, 12] in SdH experiments along with the calculated values from LDA+DMFT, LDA+U and a recent spin-polarized GW work [27]. It is apparent that LDA+U (and spin-polarized GW) strongly overestimates the splitting of all orbits, especially for the hole pockets, while a much better agreement with experiments is obtained from LDA+DMFT. The reasons for this success are: i) a proper description of the crystal-

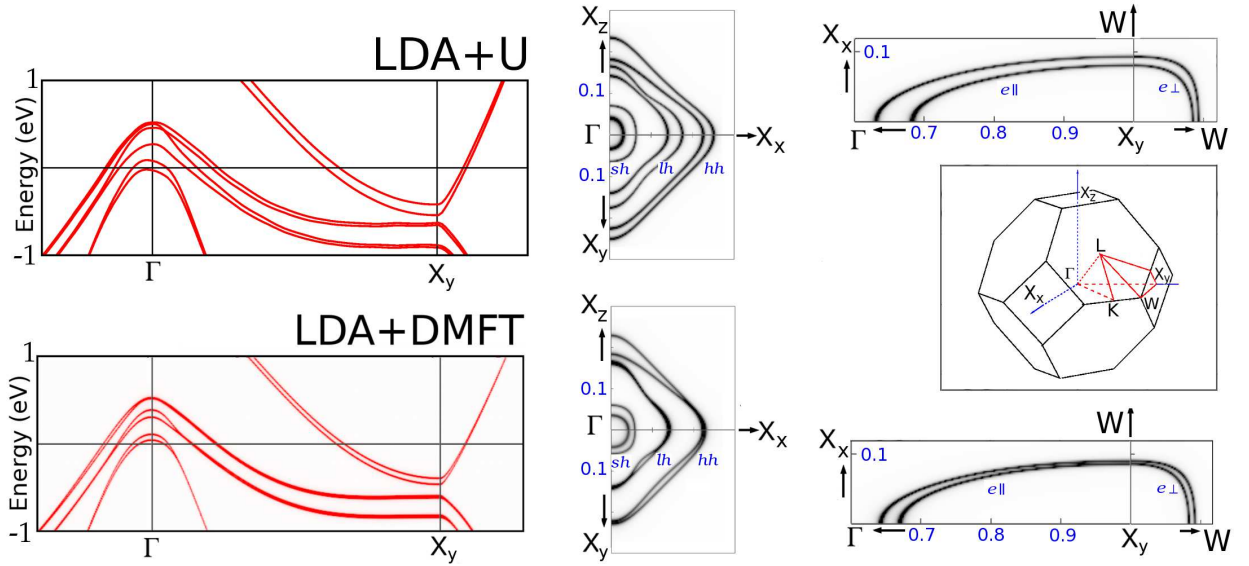


FIG. 3: (Color online) The low-energy electronic structure of ErAs within the LDA+U(top) and LDA+DMFT (bottom) approaches. The spin polarization is along the  $z$  axis, thus the cubic symmetry is lifted, and the band structure along  $x(y)$  and  $z$  axis are not equivalent. Therefore we designate the corresponding  $X$  high-symmetry points as  $X_x$ ,  $X_y$ , and  $X_z$ . The Brillouin zone is shown in insert at the right-hand side of the plot. The overlapping As  $4p$  and Er  $5d$  bands near  $E_F$  are shown on the left-hand side. They are followed to the right by the cross sections of the hole pockets at the  $\Gamma$  point in the  $xy$  and  $xz$  planes, and the longitudinal  $e \parallel$  (in the  $\Gamma X_y W$  plane) and transverse  $e \perp$  (in the  $X_y W W$  plane) cross sections of the electronic pocket. The exchange splittings of the pockets are clearly seen.

field induced freezing of the  $4f$  spin moment (in contrast to the full polarization obtained from LDA+U) and ii) a proper description of the orbital angular momentum content of the upper Hubbard band. Electronic pockets are mainly sensitive to the first effect, since the direct hybridization between the Er  $d$ - and  $f$ - states is very small near the  $X$ -point[8]. As a result, the splitting of the electronic pocket is mainly due to the exchange field induced by the polarization of the  $f$ -states in the local charge density, and hence in the effective potential seen by the  $d$ -states [28]. Because the spin polarization of the  $f$ -states is strongly overestimated in LDA+U, so is the exchange splitting of the electron pockets. In contrast, the hybridization between the As  $p$ -states and Er  $f$ -states near the  $\Gamma$ -point is rather strong. In LDA+U, the UHB has a strong spin-polarization in the minority channel: hybridization thus repels the corresponding  $p$ -states away from the Fermi level, leading to too small hole pockets in the minority channel (see Table I). In LDA+DMFT, this spin polarization is smaller and the orbital angular momentum composition of the UHB is different, with larger contributions from components which do not hybridize with  $p$ -states for symmetry reasons. Hence the smaller exchange splitting of the hole-pockets, in better agreement with experiments. It is remarkable that, because of the sensitivity of hybridization effects to both the spin and orbital angular momentum of the  $4f$  states, experimental measurements of the exchange splitting of the FS

pockets indirectly probe the electronic state of the Er  $4f$  shell.

In conclusion, we have shown that a proper description of the electronic structure of ErAs requires a conceptual framework which gives a central role to local atomic physics and multiplet effects, in contrast to conventional frameworks based on one-electron effective descriptions. This is of general importance for a wide class of materials, including all rare-earth based semiconductors and semimetals.

This work was supported by the Agence Nationale de la Recherche (France) under the ETSF Award, and by the MRSEC Program of the National Science Foundation under Award No. DMR05-20415. AG and LP thank the Chemical Bonding Center and the Kavli Institute for Theoretical Physics, UCSB, for hospitality and support. LP acknowledges the financial support from ICAM under NSF grant DMR 0645461.

- 
- [1] C. J. Palmström, N. Tabatabaie, and S. J. Allen Jr., Appl. Phys. Lett. **53**, 2608 (1988).
  - [2] K. E. Singer *et al.*, Appl. Phys. Lett. **64**, 707 (1994).
  - [3] D. O. Klenov *et al.*, Appl. Phys. Lett. **83**, 111912 (2005).
  - [4] B. D. Schultz and C. J. Palmström, Phys. Rev. B **73**, 241407(R) (2006).
  - [5] W. Kim *et al.*, Phys. Rev. Lett. **96**, 045901 (2006).

- [6] C. Kadow *et al.*, Appl. Phys. Lett. **76**, 3510 (2000).
- [7] A. G. Petukhov, W. R. L. Lambrecht, and B. Segall, Phys. Rev. B **50**, 7800 (1994).
- [8] A. G. Petukhov, W. R. L. Lambrecht, and B. Segall, Phys. Rev. B **53**, 4324 (1996).
- [9] S. J. Allen Jr. *et al.*, Phys. Rev. B **43**, 9599 (1991).
- [10] R. Bogaerts *et al.*, Physica B **177**, 425 (1992).
- [11] R. Bogaerts *et al.*, Physica B **184**, 232 (1993).
- [12] R. Bogaerts *et al.*, Phys. Rev. B **53**, 15951 (1996).
- [13] A. Georges *et al.*, Rev. Mod. Phys. **68**, 13 (1996).
- [14] D. Vollhardt *et al.*, J. Phys. Soc. Jpn. **74**, 136 (2005).
- [15] G. Kotliar *et al.*, Rev. Mod. Phys. **76**, 865 (2006).
- [16] J. Hubbard, Proc. Roy. Soc. (London) **A 276**, 238 (1963).
- [17] L. V. Pourovskii *et al.*, Phys. Rev. B **76**, 235101 (2007).
- [18] W. T. Carnal *et al.*, J. Chem. Phys. **90**, 3443 (1989).
- [19] K. R. Lea, J. M. Leask, and W. P. Wolf, J. Phys. Chem. Solids **23**, 1381 (1962).
- [20] S. J. Allen Jr. *et al.*, Phys. Rev. Lett. **62**, 2309 (1989).
- [21] V. I. Anisimov *et al.*, J. Phys. Condensed Matter **9**, 767 (1997).
- [22] P. Larson *et al.*, Phys. Rev. B **75**, 045114 (2007).
- [23] T. Komesu *et al.*, Phys. Rev. B **67**, 035104 (2003).
- [24] C. G. Duan *et al.*, Surface Review and Letters **11**, 531 (2004).
- [25] J. H. Shim, K. Haule, and G. Kotliar, Nature **446**, 513 (2007).
- [26] W. R. L. Lambrecht *et al.*, Phys. Rev. B **55**, 9239 (1997).
- [27] A. N. Chantis, M. van Schilfgaarde, and T. Kotani, Phys. Rev. B **76**, 165126 (2007).
- [28] M. Wulff *et al.*, Europhys. Lett. **7**, 629 (1988).